Torsional fatigue life evaluation for steel thin-wall specimens considering crack initiation phase

Z. Ebrahimi*[1]

Department of Mechanical Engineering, Payame Noor University (PNU), P.O.Box 19395-4697, Tehran, Iran

Abstract

In this paper, a new model for fatigue life evaluation of a steel thin-wall tubular specimen based on critical plane theory is presented. The fatigue model incorporates the crack initiation phase in the life prediction model. The total fatigue life is the sum of both crack initiation and propagation lives. Initial crack length is not applied priory, but is calculated within the model. The crack initiation life is evaluated using a critical plane approach base on a modified Smith-Watson-Topper and the Fatemi- Socie criteria. The evaluated fatigue lives are validated by experimental results for a thin-wall tubular specimen. Both critical plane criteria have resulted in similar fatigue lives, with the Fatemi-Socie criteria giving a slightly more accurate initiation life. The model absolute error is high without consideration of the crack initiation phase. The proposed model indicates that a correct determination of the fatigue life requires consideration of the crack initiation phase.

Keywords: : Steel thin-wall specimen, Initial crack length, Torsional load, Critical plane approach.

1. Introduction

Fatigue failure happens in many vehicles, aerospace and mechanical structures under cyclic loading. Many structural elements, such as hollow tubular sections and notched and circular shafts, experience fatigue. Various experimental and numerical fatigue assessment studies are reported in the literature. Ferriera et al. [1] have studied crack propagation in hollow rectangular sections and obtained the S-N curves as a function of initial crack length. Fash [2] has performed a variety of experiments to assess the fatigue behavior of smooth and notched specimens under multiaxial loading. Macdonald and Haagensen [3] investigated the fatigue properties of hollow tubes using the hot spot stress method. Pawliczek and Rozumek [4] performed fatigue tests for smooth and notched shafts under bending and torsional loading for different mean stresses.

The complex fatigue problems, under torsional and multiaxial loading, have attracted interest from many researchers. Chen et al. [5] improved the fatigue properties of a cracked rectangular hollow section using composite plates. Kashani and Cai [6] investigated the fatigue behavior and fracture of reinforcing bars under torsion. Zhao et al. [7] have proposed a new method for fatigue life prediction of steels under torsional loading. Fatemi and Molaei [8] proposed new hollow geometries for fatigue tests of additive manufactured materials. Renzo et al. [9] have suggested a modified damage model based on the Sines criterion to assess the fatigue behavior of a titanium alloy.

Hollow tubes are extensively used in mechanical engineering applications, due to their high strength-to-mass ratio. As reviewed above, many hollow and thin-wall specimens experience cyclic torsional loading. Therefore, researchers have focused more on the torsion of the hollow specimens. Ebrahimi and Negahban [10] have studied the torsion of rounded rectangular hollow tubes of functionally graded materials. Campagnolo et al. [11] have studied the torsional fatigue behavior of tube-tube steel joints using the peak stress method.

**Corresponding author*
Email: z.ebrahimi@pnu.ac.ir
Address: Mechanical Engineering Dept.
Payeme Noor University,
P.O.Box 19395-4697 Tehran, Iran.
1. Assistant Professor

On the other hand, critical plane approaches have become a successful method for fatigue life assessments under torsional and bending loadings. Bäckstörm and Marquis [12] reviewed different fatigue assessment models, including three potential damage models and a modified critical plane model for tubular welding joints under torsion. Comparing to the experimental fatigue S-N curves, they stated that the critical plane method was the most accurate model in their investigation. A multiaxial fatigue model based on a critical plane model, which can be applied to ductile and brittle materials, was developed by Wang et al. [13]. Frendo et al. [14] assessed the fatigue life of tubular welded structures under a sequence of bending and torsional loading using normal stress, notch stress and critical plane methods. He concluded that the critical plane approach determines the failure location, correctly. Ronchei and Vantadori [15] applied a critical plane approach to assess the fatigue life of a Ti-6Al-4V notched specimen under bending and torsional loading.

Most fatigue life prediction methods have assumed that the initial crack exists in the specimen priory. The crack nucleation phase is disregarded in the above-mentioned analytical models. They have mainly calculated the fatigue propagation lives. A few researchers have investigated the crack initiation fatigue lives. A failure initiation model based on Gough and Nishihara approach is reported by Khalij et al. [16] for ductile and brittle materials under cyclic bending and torsional loading. A fatigue life prediction model for a notched shaft under cyclic bending is presented by Mohammadi et al. [17]. They incorporated the crack nucleation phase into their model using a critical plane approach based on Fatemi-Socei (FS) and Smith-Watson Topper (SWT) criteria. Moreover, they proposed an algorithm for the calculation of crack depth in the specimen.

In the presented study, the crack initiation phase is incorporated into the fatigue model of thin-wall tubular specimens under cyclic torsional loading. The fatigue model is developed by applying a critical plane approach based on Fatemi-Socie and a modified Smith-Watson-Topper (WT) criteria. The initial crack is not applied priory in the specimen, but is calculated within the model. According to the experimental observations of the fatigue of hollow tubes under torsion, the crack initiates on the specimen circumference on the critical point of the stress-strain state. With this assumption, the crack length is calculated using the stress-strain time histories obtained by the Finite Element (FE) simulations. The total fatigue life combines the crack initiation and propagation lives. Consideration of the crack nucleation phase in fatigue life assessments of the tubular specimens under torsional loading has not been reported in the literature. The presented model can be adopted to evaluate the fatigue life of many tubular structures under torsional load.

2. Materials and Methods

A fatigue evaluation model is proposed for thin-wall tubes under cyclic torsion. In the presented fatigue mode, the total fatigue life is a summation of the crack initiation and propagation fatigue lives. The crack doesn't exist priory, but initiates after passing crack initiation life. The crack propagates on the outer surface of the specimens as the completely reversed torsion load is applied. The fatigue model is described in section 2.1.

The stress analysis of the thin-wall tubular specimens under cyclic torsion is performed by FE simulations. The maximum stresses and strains at the critical region of the specimen are determined for a range of torsional loading. The time histories of the stress and strain fields are evaluated on a path around the critical point. They are later inserted in the proposed algorithm for the determination of the initial fatigue life and initial crack length. The FE model is presented in section 2.2.

2.1. Fatigue life evaluation model

The total fatigue life consists of two stages; 1) The crack initiation life, N_{if}, is evaluated based on a critical plane approach using WT and FS criteria. 2) The crack propagation life, Np, is the number of cycles running after initiation of a macroscopic crack until the specimen failure. The number of cycles leading to the initiation of a macroscopic crack is presented with N_{if}. Note that in this model, the initial crack is not defined priory. The inherent imperfections and voids in the material, grow gradually as the periodic load is applied and turn into macroscopic cracks. The crack length in this model is not constant and is calculated in a similar procedure as proposed by Mohammadi et al. [17]. After the crack initiation, the propagation phase stars. The crack propagation continues until the specimen fails. The total fatigue life, N_t, is the summation of the initiation and propagation lives,

$$N_t = N_{if} + N_p \qquad \text{Eq.(1)}$$

The crack initiation phase begins with the nucleation of the crack at the critical stress region, i.e., the area with the highest stress in the specimen. In this research, the location of the critical stress in the specimen and the stress-strain state are determined using FE analysis. Inserting the stress-strain time histories into the fatigue life prediction model, the initial crack length and the initiation and propagation fatigue lives are calculated for a range of torsional loading.

2.1.1 Crack initiation life prediction

The crack initiation life is evaluated using a critical plane approach with the Fatemi-Socie and the modified Smith-Watson-Topper criteria. In critical plane theory, the fatigue evaluation is performed on a plate passing

through the critical point of the specimen, i.e., the point of the maximum stress. The FS criteria in Eq. (2) is defined in terms of the maximum shear strain amplitude, $\frac{\Delta\gamma_{max}}{2}$, and maximum normal stress, σ_{max}. In the FS criteria, the critical plane is where the parameter $\frac{\Delta\gamma_{max}}{2}$ has a maximum value.

$$\frac{\Delta\gamma_{max}}{2}\left(1+\frac{\sigma_{max}}{\sigma_y}\right)=\left(\frac{\tau'_f}{G}\right)\left(2N_{iFS}\right)^b+\gamma'_f\left(2N_{iFS}\right)^c \quad \text{Eq.(2)}$$

In the FS formula in Eq. (2), G is the shear modulus, σ_y is the yield stress, τ'_f and γ'_f are the shear fatigue and torsional ductility coefficients. The components b and c are the fatigue strength and fatigue ductility, respectively.

The Smith-Watson-Topper criteria defined in Eq. (3) is a fatigue life prediction model for dominant tensile damage problems [18]. The critical plane in this case, is the plane experiencing the maximum normal strain $\Delta\varepsilon/2$.

$$\frac{\Delta\varepsilon}{2}\sigma_{max}=\left(\frac{\sigma'^2_f}{E}\right)\left(2N_{if}\right)^2+\varepsilon'_f\sigma'_f\left(2N_{if}\right)^{b+c} \quad \text{Eq.(3)}$$

In torsional loading conditions, where the shear damage is dominant, the Smith-Watson Topper criteria can be modified as follows,

$$\frac{\Delta\gamma}{2}\sigma_{max}=C_1\left(\frac{\sigma'^2_f}{E}\right)\left(2N_{if}\right)^2+C_2\varepsilon'_f\sigma'_f\left(2N_{if}\right)^{b+c} \quad \text{Eq.(4)}$$

The coefficients C_1 and C_2 are obtained in a similar way that conventional stain-life equation is written with shear strain amplitude. The constants C_1 and C_2 are evaluated by making the two equations give the same endurance for uniaxial stresses. Following this procedure one gets $\gamma_{max}=(1+\nu)\varepsilon_1$, where ε_1 is an axial strain and ν is the Poisson's ratio [18]. Therefore, the shear strain amplitude is $(1+\nu)$ times the direct strain amplitude. Therefore, Eq. (4) can be rewritten as,

$$\frac{\Delta\gamma}{2}\sigma_{max}=(1+\nu_e)\left(\frac{\sigma'^2_f}{E}\right)\left(2N_{if}\right)^2+(1+\nu_p)\varepsilon'_f\sigma'_f\left(2N_{if}\right)^{b+c} \quad \text{Eq.(5)}$$

Elastic Poisson's ratio is 0.3 and plastic Poisson's ration is 0.5, approximately. The modified Smith-Watson-Topper criteria, which can be applied to torsion problems of ductile materials, is

$$\frac{\Delta\gamma}{2}\sigma_{max}=1.3\left(\frac{\sigma'^2_f}{E}\right)\left(2N_{iWT}\right)^2+1.5\varepsilon'_f\sigma'_f\left(2N_{iWT}\right)^{b+c} \quad \text{Eq.(6)}$$

In the above formula, The fatigue initiation life is represented by N_{if} in general. N_{iWT} and N_{iFS} are the initiation lives based on the WT and FS criteria, respectively.

In the critical plane theory, the fatigue life is calculated on all planes passing through the critical point and its smallest value, is considered as the fatigue crack nucleation life of the specimen. Fig.1. shows the schematic of the algorithm used in this study to evaluate the crack initiation fatigue life. The first step is development of the FE model to determine the relationship between the stress-strain time histories at the critical point and the applied torsional loading. The second step is the assignment of the unit normal vector passing through the critical point. The orientation of the normal vector is represented with θ,θ_r. The beginning values are $\theta=0,\theta_r=0$, and they increased with small steps to 180°. According to Eq. (7), the components of the normal vectors are calculated using the optimum values of θ and θ_r. The normal stress and normal strains are determined using Eq. (8) to Eq. (11). Theses evaluations are performed for all times in the stress-strain state. These stress-strain values are inserted in the corresponding criteria (WT and FS) and N_{if} is evaluated for all planes passing through the critical point.

$$n_x=\sin\theta\sin\theta_r$$
$$n_y=-\sin\theta\cos\theta_r \quad \text{Eq.(7)}$$
$$n_z=\cos\theta$$

$$\varepsilon_n=\varepsilon_{xx}n_x^2+\varepsilon_{yy}n_y^2+\varepsilon_{zz}n_z^2+\varepsilon_{xy}n_xn_y+\varepsilon_{yz}n_yn_z+\varepsilon_{xz}n_xn_z \quad \text{Eq.(8)}$$

$$\gamma=2\sqrt{\left(\varepsilon_r^2-\varepsilon_n^2\right)} \quad \text{Eq.(9)}$$

$$\sigma_n=\sigma_{xx}n_x^2+\sigma_{yy}n_y^2+\sigma_{zz}n_z^2+2\sigma_{xy}n_xn_y+2\sigma_{yz}n_yn_z+2\sigma_{xz}n_xn_z \quad \text{Eq.(10)}$$

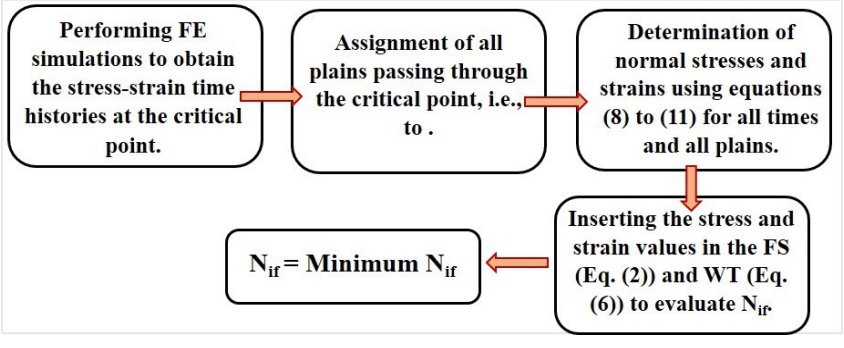

Fig. 1. A schematic of the algorithm for the evaluation of the crack initiation fatigue life.

where

$$\varepsilon_r^2 = \left(\varepsilon_x n_x + \frac{\varepsilon_{xy} n_y + \varepsilon_{xz} n_z}{2}\right)^2 + \left(\varepsilon_y n_y + \frac{\varepsilon_{yx} n_x + \varepsilon_{yz} n_z}{2}\right)^2 + \left(\varepsilon_z n_z + \frac{\varepsilon_{zx} n_x + \varepsilon_{zy} n_y}{2}\right)^2 \quad \text{Eq.(11)}$$

The minimum value of the N_{if}, evaluated on all planes, is considered as the as the crack initiation life and the corresponding plane is the critical plane.

2.1.2 Crack propagation life prediction

In the case of the thin-wall tubular specimen, the crack initiates around the specimen circumference on longitudinal shear plane [2]. Therefore, the stress and strain time histories are determined along a surfaced path around the critical point of the specimen using the FE model. A fatigue crack is nucleated when the crack propagation growth rate, $\left.\frac{da}{dN}\right|_p$, reaches the initiation growth rate, $\left.\frac{da}{dN}\right|_i$ [17]. The initial crack length can be obtained by equating these two growth rate formula. Consequently, in the proposed fatigue life assessment model, the initial crack length is not constant for different torsional loading. After evaluation of the initial crack length, the walker equation (Eq. 12) is used to determine the fatigue propagation life,

$$\left.\frac{da}{dN}\right|_p = B_1 \left(\frac{\Delta K}{(1-R)^{1-\zeta}}\right)^m \quad \text{Eq.(12)}$$

The stress intensity factor is defined in Eq. (13), where M is factor for the crack shape. For half-circle crack shape, M=0.728 is used. R is the stress ratio, which is assumed to be zero here. ΔK is the range of the stress intensity factor. The crack growth parameter $B_1 = 8.2\exp(-13)$, the growth component m=3.5 and the equivalent stress intensity factor $\zeta = 0.5$ are constant values used in the presented fatigue model.

$$\Delta K = M\Delta s\sqrt{\pi a} \quad \text{Eq.(13)}$$

Integrating Eq. (6) gives the following formula for Np,

$$\int_{N_i}^{N_f} dN = \int_{a_i}^{a_f} \frac{da}{B_1\left(\frac{M\Delta s\sqrt{\pi a}}{(1-R)^{1-\gamma}}\right)} \quad \text{Eq.(14)}$$

$$N_p = \frac{a_f^{1-m/2} - a_i^{1-m/2}}{B\left(M\Delta s\sqrt{\pi}\right)^m (1-m/2)} \quad \text{Eq.(15)}$$

Eq. (15) is used to calculate the fatigue crack propagation life, where the parameter B is defined in Eq. (16).

$$B = \frac{B_1}{(1-R)^{m(1-\gamma)}} \quad \text{Eq.(16)}$$

The final crack length, a_f is defined in Eq. (17) using mode II fracture toughness, K_{IIC}.

$$a_f = \frac{1}{\pi}\left(\frac{K_{IIC}}{Ms_{max}}\right)^2 \quad \text{Eq.(17)}$$

2.2. FE stress analysis

The FE model of the thin-wall hollow tube is developed using Abaqus software. The dimensions of the hollow tube are shown in Fig. 2. This model is based on the experimental work presented by Fash in 1985 [2]. The critical stress occurs in the middle of the tube, where it has the minimum thickness. One end of the tube is placed in the testing machine and the torsional loading is applied at the other end. The torsional fatigue test is controlled by adjusting the strain value. Finally, the test is stopped after observation of the macroscopic crack and the failure of the specimen. As the torsional strain increases, the initial crack length gets longer.

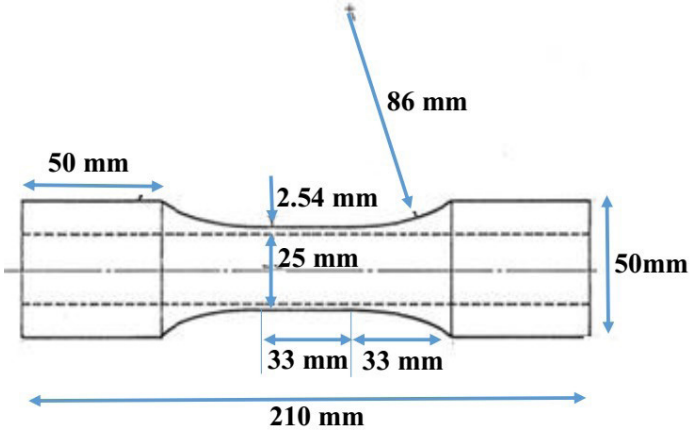

Fig. 2. The thin-wall tube specimen used for cyclic torsional tests [2].

The FE model and the FE mesh of the thin-wall tube are presented in Fig. 3. The mesh size is 3 mm. The element number is 12212 and the number of nodes is 15480. The element type is C3D8R, which is a cubic-8-node element. The torsional loading is applied at a reference point (RP) defined at the end of the tube.

4. Results and Discussions

4.1. Results of the FE stress analysis

The results of the FE stress analysis are presented here. The von-mises stress distribution is presented in Fig. 4. The applied torsional load for this simulation is T=1400 N.m. The maximum stress occurs at the central region of the specimen, with a maximum value of $\Delta\sigma_{max} = 380$ MPa .

A convergence and mesh refinement study is performed to show that the FE model and results are independent of the mesh. For this reason, the maximum stress at the critical point of the thin-wall tube is determined for three different element sizes, 2.5, 3 and 5 mm. As illustrated in Fig. 5, the maximum stress is converged for 3 mm element size. This value is used for the rest of the simulations in the study.

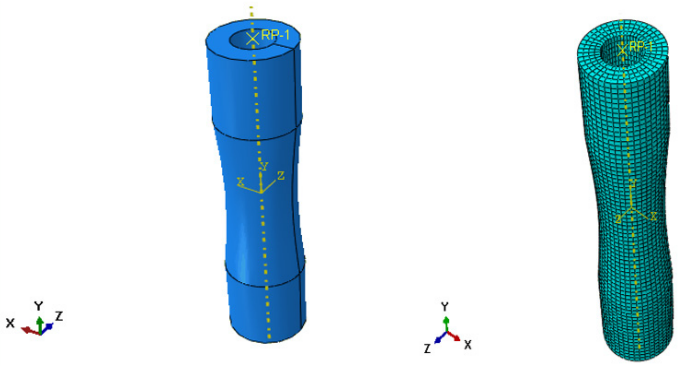

Fig. 3. The FE model of the tubular specimen under cyclic torsional loading.

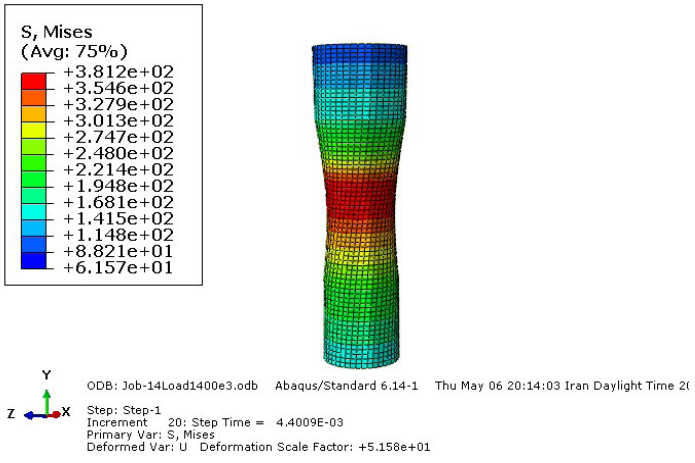

Fig. 4. The stress distribution of the thin-wall tube under cyclic torsion.

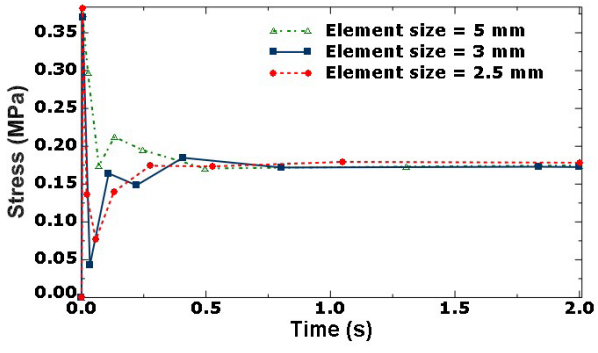

Fig. 5. Mesh refinement study for the FE stress analysis.

Next, the maximum strains at the critical point of the thin-wall tube are determined. The time histories of the shear strains $\varepsilon_{12}, \varepsilon_{23}$ and the maximum principal strain are plotted in Fig. 6. The maximum strain for T=1400 N.m is 2.4e-3. The shear stress components and the von-mises stress at the critical region of the thin-wall tube are also plotted in Fig. 7 for T=1400 N.m, where the maximum stress is $\Delta\sigma_{max} = 380$ MPa .

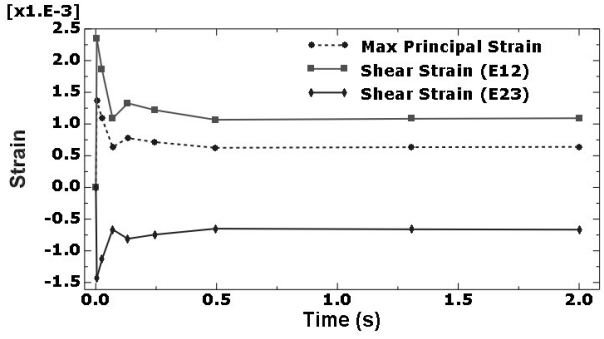

Fig. 6. The shear strain components and the maximum principal strain at the critical region of the thin-wall tube under cyclic torsion.

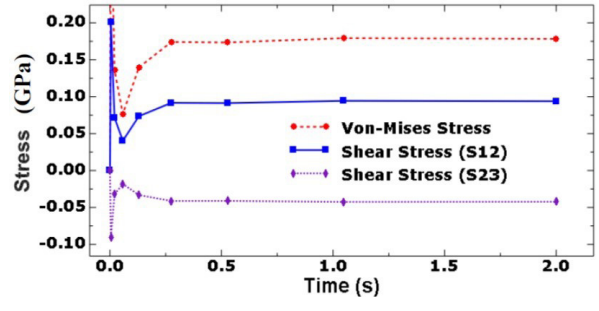

Fig. 7. The shear stress components and the von-mises stress at the critical region of the thin-wall tube under cyclic torsion.

4.2. Results of the fatigue life evaluation model

In this section, the results of the fatigue life prediction model for the thin-wall tubular specimen under cyclic torsional loading are presented. As stated before, the total fatigue life in the presented model, is the summation of the crack initiation and the crack propagation lives. There was no need for defining the initial crack priory in this model. However, the crack was initiated after applying the cyclic loading and the initial crack length was calculated using the stress-strain state at the critical point of the specimen. The initial crack length depends on the loading range and the critical stress-strain state.

To validate the calculated fatigue lives, the numerical results are compared with the experimental investigations performed by Fash [2]. The material used in the fatigue experiments is SAE-1045 steel. Some mechanical properties of SAE-1045 steel and some fatigue model parameters are given in Table 1.

The fatigue life evaluation model, is implemented in a piece of Matlab code and is linked with the FE stress-strain state results. The fatigue lives are evaluated for strain levels of 0.15, 0.22, 0.4 and 1.0 percent and are compared with experimental results of Ref. [2]. The predicted and experimental fatigue lives are reported in Table 2. Experimental results and the evaluated total fatigue lives, obtained by WT and FS initial life criteria, are in good correlation.

The maximum stress and strains are presented in the first and second columns of Table 2. N_{iWT} and N_{iFS} are the calculated initial lives base on WT and FS criteria, respectively. The fatigue propagation lives are evaluated with different initial crack lengths. The computed crack lengths are presented in the 6th column. The Total predicted fatigue lives are reported on seventh and eight columns of Table1. The total fatigue lives are the combination of the initiation and propagation lives, i.e. $N_{WT} = N_{iWT} + N_p$ and $N_{FS} = N_{iFS} + N_p$.

For the maximum range of the critical stresses $\Delta\sigma_{max} = 502$ MPa and $\Delta\sigma_{max} = 294$ MPa , the initial crack lengths are $a_i = 998$ μm and 50 μm respectively. The predicted fatigue lives for both WT and FS criteria are plotted versus experimental lives in a logarithmic scale in Fig. 8. The evaluated results are in

Table 1. Mechanical properties of the SAE-1045 steel in the fatigue tests.

E (GPa)	σ_y (MPa)	σ_U (MPa)	σ'_f (MPa)	ε'_f	τ'_f (MPa)	γ'_f (MPa)	b	c	m	
205	380	621	809	0.173	0.528	0.35	-0.1	-0.468	3.5	0.5

Table 2. Comparing experimental results and the evaluated total fatigue lives.

$\Delta\sigma_{max}$ (MPa)	$\Delta\varepsilon_{max}$	N_{iWT}	N_{iFS}	N_p	a_i (μm)	WT - predicted N_{WT}	FS - predicted N_{FS}	Experimental N_T
502	17.3e-3	617	330	580	998	1,197	910	890
394	7.2e-3	6,970	4,703	4,703	970	11,044	8,776	8710
336	3.81e-3	52,955	48,155	76,011	167	128,970	124,170	102,083
294	2.6e-3	652,610	711,210	406,740	50	873,508	932,118	1,010,210

excellent agreement with fatigue tests. The fatigue lives without consideration of the crack initiation phase, i.e. N_p, are also plotted in Fig. 8 as well. The effects of the stress state on the predicted fatigue lives are illustrated in Fig. 9. Obviously, the FS model has the best performance in the prediction of thin-wall tube fatigue lives under cyclic torsional loading.

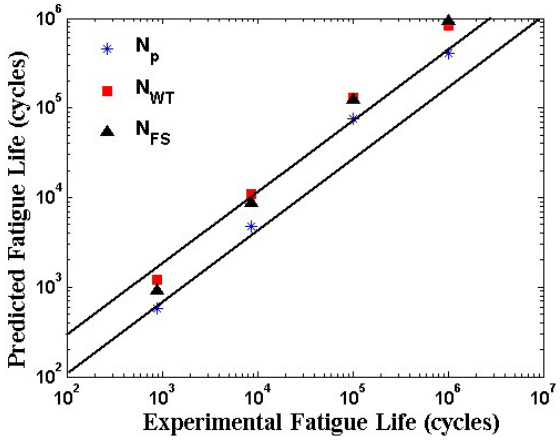

Fig. 8. The predicted total fatigue lives versus experimental results.

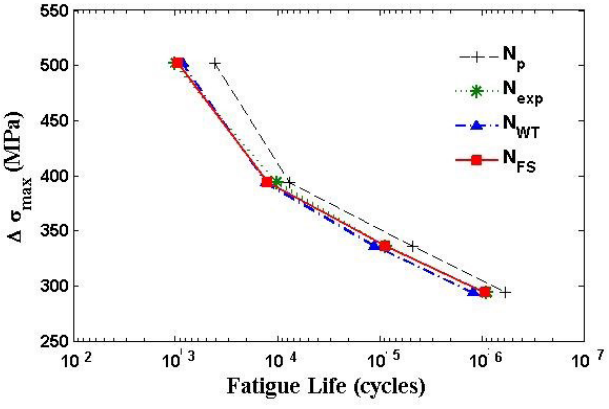

Fig. 9. Experimental and evaluated fatigue lives versus maximum stress range.

The error of the numerical model is defined in Eq. (18), where e_i is the error-index for the fatigue life in each stress state. The average absolute error, $\bar{e}$, is the average of the error indices [17].

$$e_i = \log\left(\frac{N_{fi}}{N_{exp}}\right), \bar{e} = \frac{1}{n}\left(\sum_{i=1}^{n} | e_i |\right) \qquad \text{Eq.(18)}$$

The values of error index versus maximum stress range for fatigue life prediction models, including crack initiation phase based on WT and FS criteria, are shown in Fig. 10. The error indices for N_p, which is obtained without consideration of the initial crack lengths, are also presented in Fig. 11.

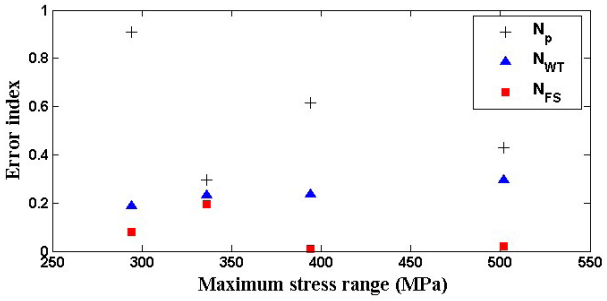

Fig. 10. Error index versus maximum stress range for fatigue life prediction models.

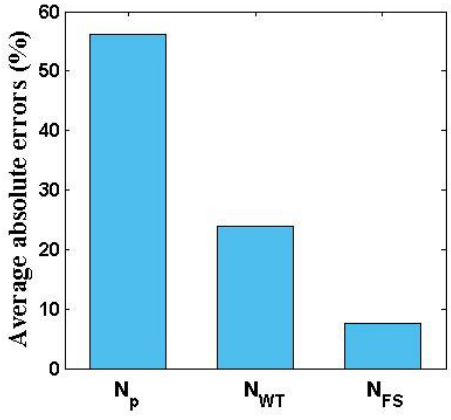

Fig. 11. The average absolute errors for the fatigue lives with and without crack initiation phase.

The average absolute error for the models, including crack initiation life is 7.65% for FS and 23.88% for WT criteria. The average error for the model without considering the crack nucleation life is 56.23% for the thin-wall tube model. Without consideration of crack the initiation phase, the error of the absolute error is high. The proposed model indicates that a correct determination of the fatigue life requires consideration of crack initiation phase.

An improved model for fatigue life evaluation of thin-wall tubular structures based on critical plane theory is presented. This new fatigue model incorporates the crack initiation phase in the life prediction model. The total fatigue life is a combination of both crack initiation and crack propagation lives. The initial crack length is not applied priory, but is calculated within the model. The crack initiation life is evaluated using a critical plane approach base on a modified Smith-Watson-Topper (WT) and the Fatemi-Socie (FS) criteria. The fatigue lives obtained from the proposed model are validated by experimental results for a thin-wall tubular specimen. Both critical plane criteria gave similar fatigue lives, with the FS criteria giving a slightly more accurate initiation life. Without consideration of crack initiation phase, the model absolute error is high. The proposed model indicates that a correct determination of the fatigue life requires consideration of crack initiation phase.

4. Conclusions

In this study, the crack initiation phase was incorporated into the fatigue model of thin-wall tubular specimens under cyclic torsional loading. The fatigue model was developed by applying a critical plane approach based on two different criteria, FS and WT. The advantage of this model was the calculation of the initial crack length considering circumferential crack nucleation. The crack length was determined using the stress-strain time histories obtained by the FE analysis. The total fatigue life was a summation of the crack initiation and propagation lives. The predicted fatigue lives were validated by experimental results for a thin-wall tubular specimen. Both critical plane criteria gave similar fatigue lives, with the Fatemi-Socie criteria giving a slightly more accurate initiation life. Without incorporating the crack nucleation phase, the absolute error of the predicted fatigue lives was relatively high. The proposed model indicates that a correct determination of the fatigue life requires consideration of the crack initiation phase.

References

[1] J. A. Ferreira, C. M. Branco, J. C. Radon, Fatigue life assessment in welded rectangular hollow sections using fracture mechanics, Application of Fracture Mechanics to Materials and Structures. (1984) 749-761. https://doi.org/10.1007/978-94-009-6146-3_51

[2] Fash JW. An evaluation of damage development during multiaxial fatigue of smooth and notched specimens. In: Material engineering report no 123. University of Illinois at Urbana-Champaigne (1985).

[3] K.A. Macdonald, P.J. Haagensen, Fatigue of welded aluminium hollow section profiles, Engineering Failure Analysis. 16 (2009) 254–261. https://doi.org/10.1016/j.engfailanal.2008.03.004

[4] R. Pawliczek, D. Rozumek, Cyclic Tests of Smooth and Notched Specimens Subjected to Bending and Torsion Taking into Account the Effect of Mean Stress, Materials. 13(9) (2020) 2141. https://doi.org/10.3390/ma13092141

[5] T. Chen., X. Wang, M. Qi, Fatigue improvements of cracked rectangular hollow section steel beams strengthened with CFRP plates, Thin-Walled Structures. 122 (2018) 371–377. https://doi.org/10.1016/j.tws.2017.10.019

[6] M. M. Kashani, S. Cai, S. A. Davis, P. J. Vardanega, Influence of Bar Diameter on Low-Cycle Fatigue Degradation of Reinforcing Bars, Journal of Materials in Civil Engineering 31(4) (2019) 06019002. https://doi.org/10.1061/(asce)mt.1943-5533.0002637

[7] E. Zhao, Q. Zhou, W. Qu, W. Wang, Fatigue Properties Estimation and Life Prediction for Steels under Axial, Torsional, and In-Phase Loading, Advances in Materials Science and Engineering. (2020) 1-8. https://doi.org/10.1155/2020/8186159

[8] A. Fatemi, R. Molaei, Novel specimen geometries for fatigue testing of additive manufactured metals under axial, torsion, and combined axial-torsion loadings, International Journal of Fatigue. 130 (2020) 105287. https://doi.org/10.1016/j.ijfatigue.2019.105287

[9] D. A. Renzo, E. Sgambitterra, C. Maletta, F. Furgiuele, C. A. Biffi, J. Fiocchi, A. Tuissi, Multiaxial fatigue behavior of SLM Ti6Al4V alloy under different loading conditions, Fatigue & Fracture of Engineering Materials & Structures. 2021;1–18. https://doi.org/10.1111/ffe.13518

[10] Z. Ebrahimi, S. Negahban, Investigation of Stress Concentration Factors for Functionally Graded Hollow Tubes with Curved Edges under Torsion, Iranian Journal of Materials Forming. 8(2) (2021) 22-34. https://doi:10.22099/ijmf.2021.39443.1175

[11] A. Campagnolo, M. Vormwald, E. Shams, G. Meneghetti, Multiaxial fatigue assessment of tube-tube steel joints with weld ends using the peak stress method. International Journal of Fatigue. 135 (2020) 105495. https://doi.org/10.1016/j.ijfatigue.2020.105495

[12] M. Bäckstörm, G. Marquis, A review of multiaxial fatigue of weldments: experimental results, design code and critical plane approaches, Fatigue & Fracture of Engineering Materials & Structures. 24(5) (2001) 279–291. https://doi.org/10.1046/j.1460-2695.2001.00284.x

[13] C. Wang, D. G. Shang, X.W. Wang, A new multiaxial high-cycle fatigue criterion based on the critical plane for ductile and brittle materials, Journal of Materials Engineering and Performance. 24(2) (2015) 816-824. https://doi.org/10.1046/j.1460-2695.2001.00284.x

[14] F. Frendo, G. Marulo, A. Chiocca, L. Bertini, Fatigue life assessment of welded joints under sequences of bending and torsion loading blocks of different lengths, Fatigue & Fracture of Engineering Materials & Structures. 43(6) (2020) 1290-1304. https://doi.org/10.1111/ffe.13223

[15] C. Ronchei, S. Vantadori, Notch fatigue life estimation of Ti-6Al-4V, Engineering Failure Analysis. 120 (2021) 105098. https://doi.org/10.1016/j.engfailanal.2020.105098

[16] L. Khalij, E. Pagnacco, R. Troian, Fatigue criterion improvement of Gough and Nishihara & Kawamoto to predict the fatigue damage of a wide range of metallic materials, International Journal of Fatigue. 99 (2017) 137–150. https://doi.org/10.1016/j.ijfatigue.2017.02.016

[17] M. Mohammadi, M. Zehsaz, S. Hassanifard, A. Rahmatfam, An evaluation of total fatigue life prediction of a notched shaft subjected to cyclic bending load. Engineering Fracture Mechanics. 166 (2016) 128-138. https://doi.org/10.1016/j.engfracmech.2016.08.027

[18] Y. L. Lee, M. E. Barkey, H. T. Kang, Metal fatigue analysis handbook: practical problem-solving techniques for computer-aided engineering, Elsevier Inc, 2012